This article has been accepted for publication in a future issue of this journal, but has not been fully edited. Content may change prior to final publication. Citation information: DOI 10.1109/TAC.2021.3077457, IEEE Transactions on Automatic Control

A Distributed Active Perception Strategy for Source Seeking and Level Curve Tracking

Said Al-Abri, *Member, IEEE,* and Fumin Zhang, *Senior Member, IEEE*

***Abstract*—Algorithms for multi-agent systems to locate a source or to follow a desired level curve of spatially distributed scalar fields generally require sharing field measurements among the agents for gradient estimation. Yet, in this paper, we propose a distributed active perception strategy that enables swarms of various sizes and graph structures to perform source seeking and level curve tracking without the need to explicitly estimate the field gradient or explicitly share measurements. The proposed method utilizes a consensus-like Principal Component Analysis perception algorithm that does not require explicit communication in order to compute a local body frame. This body frame is used to design a distributed control law where each agent modulates its motion based only on its instantaneous field measurement. Several stability results are obtained within a singular perturbation framework which justifies the convergence and robustness of the strategy. Additionally, efficiency is validated through robots experiments.**

I. Introduction

An important problem in swarm robotics is the deployment of multiple robots in order to achieve source seeking or level-curve tracking behaviors in a scalar field. In source seeking problems, agents are tasked with finding the location that minimizes or maximizes the scalar field while in level-curve tracking, agents are tasked with tracking a trajectory that achieves a constant field value. The field can represent environmental characteristics such as chemical concentrations, light intensities, or heat. These two problems have various applications including environmental monitoring, source signal localization, exploration, hazardous regions mapping, and search and rescue [16], [17], [20], [25], [27].

The dual problems of source seeking and level curve tracking have been extensively studied in the literature. In [6], [8], [15], [32], agents exchange field measurements to estimate and climb the field gradient. A gradient-based strategy is presented in [31] where agents split into subgroups that each steer towards a source. Alternatively, solutions based on extremum control are developed for one agent in [12], [13] and for multiple agents in [21], [24]. Although extremum control is simple to implement, the agents still need to exchange some estimated parameters. A cooperative control law is designed in [33] for two agents such that one agent estimates the field gradient and the other one follows it. Independent of gradient estimation, algorithms are designed in [9], [10] for a 2-agent system but require communicating field measurements. Relying on communication channels to share measurements is practically challenging such as in underwater mobile sensor networks [22].

Inspired by a school of fish seeking darker areas [7], the Speeding-Up and Slowing-Down (SUSD) strategy is developed for source seeking without gradient estimation in [35] and [34] for 2-D and 3-D environments, respectively. The SUSD strategy requires a common motion direction that can be computed locally and without explicit communication only for 2-agent and 3-agent systems in 2-D and 3-D, respectively. Differently, in [2] we used a leader-follower consensus-on-a sphere to obtain the common motion direction where agents are assumed to be able to measure the velocity directions of their neighbors.

In this paper, we propose a distributed strategy composed of two layers for perception and control. In the perception layer, each agent uses the relative positions of its neighbors to learn a geometric body frame. In the control layer, each agent modulates its motion based on the body frame and a locally measured environmental field value. The interplay between the two layers results in an indirect distributed active perception strategy where the controlled behavior of the agents enhances the information contents of the instantaneous measurements of the field and relative positions. The strategy enables a swarm to perform collective source seeking and level curve tracking of scalar fields without the need to explicitly estimate the field gradient or explicitly exchange field measurements.

The primary novelty of this work is in utilizing the Oja Principal Component Analysis (PCA) flow [5], [29], [36] to agree on a frame to coordinate the motion. This allows us to solve the main challenge in this paper which is to design a motion direction that all agents compute locally without communication. The PCA perception algorithm works as a consensus law with an input formed by the covariance of the relative positions of the neighboring agents. This is different than the existing consensus laws where the input is formed by the headings of neighbors [26]. Additionally, the PCA perception algorithm captures the changes in the spatial shape and orientation of the swarm, which represents an indirect feedback signal of how the field is affecting the motions of other agents. Since the relative positions are locally measured, then the PCA flow achieves consensus without requiring the agent to exchange data among them.

The first contribution of this paper is utilizing a PCA perception algorithm on relative positions to achieve a consensus in the body frame. The second contribution is a distributed control law that accomplishes both the missions of source seeking and level curve tracking. The third contribution is deriving the information dynamics, not only for source seeking and level curve tracking but for general control laws. The fourth contribution is obtaining input-to-state stability results

Said Al-Abri and Fumin Zhang are at School of Electrical and Computer Engineering, Georgia Institute of Technology, Atlanta, GA 30332, E-mail: {saidalabri,fumin}@gatech.edu.

within a singular perturbation framework analysis for (1) the convergence of the SUSD search direction to the negative gradient direction, and (2) the convergence of the swarm trajectory to the source location or to the desired level curve. The last contribution is validating the proposed strategy via experiments conducted via the Georgia Tech Robotarium [30] and the Georgia Teach Miniature Autonomous Blimps [11].

Preliminary results of this paper appear in our two conference papers [1], [3]. In this paper we derive the information dynamics for a generic control law within a distributed active perception algorithm that has not been introduced in [1], [3]. As a significant difference, in this paper we do consider the nonlinearities of the field in both the dynamics derivation and convergence analysis, which are ignored in [1], [3]. This allows us to refine the convergence neighborhood around the desired equilibrium. Additionally, while in [1], [3] we only proved that the SUSD direction converges to the negative gradient direction, in this paper, we also prove that the swarm converges to either the source location or the desired level curve. Furthermore, the conference papers do not include any experimental results. A longer preprint of this paper can be accessed in [4], which contains a generalization of the control laws and analysis to incomplete graphs.

II. Problem Formulation

Consider a swarm of M agents each located at position $\boldsymbol{r}_i \in \mathbb{R}^2$. The interaction between the agents is described by an undirected visibility graph, $\mathcal{G} \subseteq \mathcal{V} \times \mathcal{E}$ where $\mathcal{V}$ is the set of all agents, and $\mathcal{E}$ is the set of all edges. We consider the following assumption.

Assumption II.1. *The graph $\mathcal{G} \subseteq \mathcal{V} \times \mathcal{E}$ is undirected and complete. i.e. $(i,j) \in \mathcal{E}$ and $(j,i) \in \mathcal{E}$ for all $\{(i,j) \in \mathcal{E}\}$.*

A generalization of the control laws and analysis to incomplete graphs is available in a longer preprint of this paper which can be accessed in [4].

Assumption II.2. *Each i-th agent knows the relative positions $(\boldsymbol{r}_j - \boldsymbol{r}_i)$ for all $j \neq i$.*

In practice, robots can be equipped with sensors to measure the relative positions of their neighbors with respect to their local frame, which is less challenging than requiring the global positions [28].

Furthermore, suppose there exists a scalar field $z : \mathbb{R}^2 \to \mathbb{R}$. The analytical expression of the field function z is not known, but each agent can only measure its value $z(\boldsymbol{r}_i)$ at its current position $\boldsymbol{r}_i(t)$.

Assumption II.3. *The field is assumed to be real analytic, time-invariant and bounded, i.e. $0 \leq z(\boldsymbol{r}_i) \leq z_{max}$, and has a unique minimum at the source location $\boldsymbol{r}_0$ where $z(\boldsymbol{r}_0) = 0$.*

We require smoothness because later we design the speed of each agent to be proportional to the field measurement. However, non-smooth fields might be transformed into smooth fields using, for example, stochastic modeling, as in [34]. The field needs to be real analytic, so in the convergence analysis we can apply Taylor approximation.

Consider $z^d \in \mathbb{R}$ to be a desired level curve field value, where a level curve is the set $\{\boldsymbol{r} | z(\boldsymbol{r}) = z^d, \forall r \in \mathbb{R}^2\}$.

Assumption II.4. *The desired level curve $\{\boldsymbol{r} | z(\boldsymbol{r}) = z^d\}$ is connected.*

Finally, let the motion of each agent be described by

$$\dot{\boldsymbol{r}}_i = \frac{d\boldsymbol{r}_i}{dt} = \boldsymbol{u}_i, \quad i = 1, \cdots, M, \tag{1}$$

where $\boldsymbol{u}_i$ is a local control law to be designed.

Problem Statement. *Without explicitly estimating the field gradient and without explicitly communicating field measurements, design the local control law $\boldsymbol{u}_i$, such that the swarm autonomously steers towards either the source location $\boldsymbol{r}_0$, or the desired level curve $\{\boldsymbol{r} | z(\boldsymbol{r}) = z^d, \forall r \in \mathbb{R}^2\}$, and keeps tracking it.*

III. The Distributed Active Perception Strategy

We propose a strategy that is composed of two layers for perception and control as illustrated in Fig. 1. In the perception layer, each agent learns from the relative positions a time-varying locally computed body frame. The motion of each agent is designed in the control layer based on the perceived body frame and the locally measured environmental field value. The interplay between the two layers results in an active perception of the spatial gradient of the environmental property. In what follows, we first present the perception algorithm and then the distributed control law.

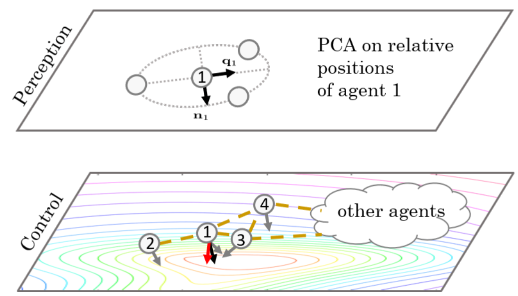

Fig. 1: The two layers of the active perception strategy.

A. The PCA Perception Algorithm

Let each computes the covariance matrix $\boldsymbol{C}(t) \in \mathbb{R}^{2\times 2}$ given by

$$\boldsymbol{C}(t) = \sum_{k=1}^{M} \big(\boldsymbol{r}_k(t) - \boldsymbol{r}_c(t)\big)\big(\boldsymbol{r}_k(t) - \boldsymbol{r}_c(t)\big)^{\mathsf{T}}, \tag{2}$$

where $\boldsymbol{r}_c = \frac{1}{M}\sum_{k=1}^{M} \boldsymbol{r}_k$ is the center of the swarm. Principal Component Analysis (PCA) computes the directions of maximum (minimum) variation of a data set [18]. Applying PCA on the covariance matrix (2), each agent locally computes the eigenvectors $\boldsymbol{q}(t)$ and $\boldsymbol{n}(t)$ of (2) corresponding to the largest and smallest eigenvalues, λ^q and λ^n, respectively. The eigenvectors $\boldsymbol{q}(t)$ and $\boldsymbol{n}(t)$ represent the direction of the maximum and minimum variances of the data, with the eigenvalues giving the variances of the data along each direction. We define the PCA body-frame to be $(\boldsymbol{q}(t), \boldsymbol{n}(t))$, where $\boldsymbol{q}(t)$ and $\boldsymbol{n}(t)$ are orthonormal vectors in $\mathbb{R}^2$.

Let $(\hat{\boldsymbol{q}}, \hat{\boldsymbol{n}})$ be an estimate of the true PCA body-frame $(\boldsymbol{q}(t), \boldsymbol{n}(t))$, which is given by the Oja PCA flow [5], [36]

$$\frac{d\hat{\boldsymbol{q}}}{d\tau} = (\boldsymbol{I} - \hat{\boldsymbol{q}}\hat{\boldsymbol{q}}^{\mathsf{T}})\boldsymbol{C}(t)\hat{\boldsymbol{q}}, \quad \hat{\boldsymbol{n}} = \boldsymbol{R}\hat{\boldsymbol{q}}, \tag{3}$$

where $\boldsymbol{R}$ is a 90° counterclockwise rotation matrix. Observe that we use the argument τ instead of t to emphasize that for any given covariance matrix $\boldsymbol{C}(t)$ at time instant t, agent i runs (3) at a different time scale τ.

Assumption III.1. *For the covariance matrix (2),* $\lambda^q \neq \lambda^n$.

This is to ensure the eigenvectors $\boldsymbol{q}$ and $\boldsymbol{n}$ are uniquely defined which ensures the mathematical correctness of the derived dynamics and convergence results obtained in this paper. In practice, due to sensing errors on measuring relative positions, it is unlikely to have $\lambda^q = \lambda^n$.

B. The Distributed Active Perception Control Law

Given the PCA body frame $(\boldsymbol{q}(t), \boldsymbol{n}(t))$ obtained by (3), we propose the control law

$$\boldsymbol{u}_i(t) = k_1(z_i(t) - z^d)\boldsymbol{n}(t) + k_2\boldsymbol{q}(t), \tag{4}$$

where $z_i(t)$ and z^d are the measured and desired field values, respectively. The parameters $k_1, k_2 \in \mathbb{R}$ are positive tuning parameters. To intuitively explain the control law (4), we simulate it in Fig. 2 for a 2-agent system in a scalar field. In this example, $\boldsymbol{q}$ is along the line-of-sight between the two agents, and $\boldsymbol{n}$ is perpendicular to the line-of-sight. When $z^d = 0$ and $k_2 = 0$, then agent i speeds up or slows down along the direction $\boldsymbol{n}$ depending on the local field measurement $z_i(t)$. Since the two agents are moving in the same direction at different speeds, then eventually they steer towards the minimum of the field. On the other hand, when $z^d \neq 0$ and $k_2 = 0$, the two agents approach the level curve $\{\boldsymbol{r} | z(\boldsymbol{r}_1) = z(\boldsymbol{r}_2) = z^d\}$. Finally, when $z^d \neq 0$ and $k_2 \neq 0$, then the first term $k_1(z_i(t) - z^d)\boldsymbol{n}(t)$ steers the 2-agent system towards the desired level curve, while the second term $k_2\boldsymbol{q}(t)$ moves the swarm along the level curve.

Remark 1. *The PCA flow* $\frac{d\boldsymbol{q}_i}{d\tau} = (\boldsymbol{I} - \boldsymbol{q}_i(\tau)\boldsymbol{q}_i^\mathsf{T}(\tau))\boldsymbol{C}\boldsymbol{q}_i(\tau)$ *can be viewed as a consensus law. However, its input is the local covariance* $\boldsymbol{C}$*, not the sum of headings* $\sum_{j\in\mathcal{N}_i}\boldsymbol{q}_j$ *as in the classical consensus law* $\dot{\boldsymbol{q}}_i = (\boldsymbol{I} - \boldsymbol{q}_i\boldsymbol{q}_i^\mathsf{T})\sum_{j\in\mathcal{N}_i}\boldsymbol{q}_j$ *which requires agents to communicate* $\boldsymbol{q}_j$*. Therefore, agents can agree on a common direction by only observing local positions. Additionally, the solution of the PCA consensus is determined by the environmentally-driven positions of the agents which is different than the heading consensus where the agreement is solely dependent on the initial headings.*

IV. The Information Dynamics

Let $z_c^d = z_c - z^d$ where z_c is the field measurement at the center $\boldsymbol{r}_c = \frac{1}{M}\sum_{l=1}^M \boldsymbol{r}_l$. Define $\boldsymbol{N}_c = \nabla z(\boldsymbol{r}_c)/\|\nabla z(\boldsymbol{r}_c)\|$ to be a unit-length vector along the direction of the field gradient at the center $\boldsymbol{r}_c$. Then, using (1) and (4), we obtain

$$\dot{z}_c^d = \frac{\|\nabla z_c\|}{M}\sum_{l=1}^M [k_1(z_l - z^d)\langle \boldsymbol{N}_c, \boldsymbol{n}\rangle + k_2\langle \boldsymbol{N}_c, \boldsymbol{q}\rangle]. \tag{5}$$

Observe that $z_c^d \to 0$ if and only if $z_c \to z^d$ for the level curve tracking, or $z_c \to 0$ for the source seeking. However, to analyze the convergence of the origin $z_c^d = 0$ of (5), we need the dynamics of the two principle directions $(\dot{\boldsymbol{q}}, \dot{\boldsymbol{n}}) = (\frac{d\boldsymbol{q}}{dt}, \frac{d\boldsymbol{n}}{dt})$.

Remark 2. *The dynamics* $(\frac{d\boldsymbol{n}}{dt}, \frac{d\boldsymbol{q}}{dt})$ *are different from* $(\frac{d\hat{\boldsymbol{n}}}{d\tau}, \frac{d\hat{\boldsymbol{q}}}{d\tau})$ *given by the PCA flow (3), which describes the dynamics of learning the body frame from a given covariance matrix* $\boldsymbol{C}(t)$ *at time instant* t.

In what follows we derive the dynamics of the body frame $(\dot{\boldsymbol{q}}, \dot{\boldsymbol{n}})$ first for a general control law $\boldsymbol{u}_l$, and then for the proposed control law (4).

The following result presents the dynamics of the PCA body frame for a general control law, $\boldsymbol{u}_i$.

Lemma IV.1. *Let Assumption III.1 holds. Then, when the agents move according to (1), the dynamics of the body frame are*

$$\dot{\boldsymbol{n}} = -\kappa\boldsymbol{q}, \quad \dot{\boldsymbol{q}} = \kappa\boldsymbol{n}, \tag{6}$$

where $\kappa = \frac{1}{\lambda^q - \lambda^n}\sum_{k=1}^M \langle \boldsymbol{q}, \boldsymbol{u}_k\rangle\langle \boldsymbol{r}_k - \boldsymbol{r}_c, \boldsymbol{n}\rangle + \frac{1}{\lambda^q - \lambda^n}\sum_{k=1}^M \langle \boldsymbol{q}, \boldsymbol{r}_k - \boldsymbol{r}_c\rangle\langle \boldsymbol{u}_k, \boldsymbol{n}\rangle$.

See proof in Section VIII. It is interesting to observe that the actions of the neighbors in $\boldsymbol{u}_k$ are present in (6) not due to communication, but due to the distributed active perception algorithm where the body frame is obtained via the PCA (3).

We then derive the dynamics of the body frame under the proposed control law (4).

Lemma IV.2. *Let Assumption III.1 holds. Then, using the motion dynamics (1) along with the control law (4), the dynamics of the body frame for source seeking and level curve tracking with complete graphs are*

$$\dot{\boldsymbol{n}} = -k_1\frac{1}{\lambda^q - \lambda^n}\boldsymbol{w}^\mathsf{T}\boldsymbol{q}\boldsymbol{q}, \tag{7}$$

$$\dot{\boldsymbol{q}} = k_1\frac{1}{\lambda^q - \lambda^n}\boldsymbol{w}^\mathsf{T}\boldsymbol{q}\boldsymbol{n}, \tag{8}$$

$$\boldsymbol{w} = \sum_{k=1}^M (z_k - z_c)(\boldsymbol{r}_k - \boldsymbol{r}_c). \tag{9}$$

See proof in Section VIII. To find the relationship between $\boldsymbol{n}$ and the gradient ∇z_c, we approximate the measurement $z_k = z(\boldsymbol{r}_k)$ by Taylor expansion with respect to the center $\boldsymbol{r}_c$. Since according to Assumption II.3 the field function z is analytic, then we can write

$$z_k - z_c = \langle \boldsymbol{r}_k - \boldsymbol{r}_c, \nabla z_c\rangle + \nu_k, \tag{10}$$

where $\nabla z_c = \nabla z(\boldsymbol{r}_c)$ is the gradient in the vicinity of the center $\boldsymbol{r}_c$, and $\nu_k = \mathcal{O}\|\boldsymbol{r}_k - \boldsymbol{r}_c\|$ represents the higher-order terms.

Then, we obtain the following result.

Lemma IV.3. *Let Assumption II.3 and Assumption III.1 hold. Then, using the motion dynamics (1) along with the control law (4), the dynamics of the body frame for source seeking and level curve tracking with complete graphs are*

$$\dot{\boldsymbol{n}} = -k_1\|\nabla z_c\|\frac{\lambda^q}{\lambda^q - \lambda^n}\langle \boldsymbol{N}_c, \boldsymbol{q}\rangle\boldsymbol{q} - \hat{\nu}\boldsymbol{q}, \tag{11}$$

$$\dot{\boldsymbol{q}} = +k_1\|\nabla z_c\|\frac{\lambda^q}{\lambda^q - \lambda^n}\langle \boldsymbol{N}_c, \boldsymbol{q}\rangle\boldsymbol{n} + \hat{\nu}\boldsymbol{n}, \tag{12}$$

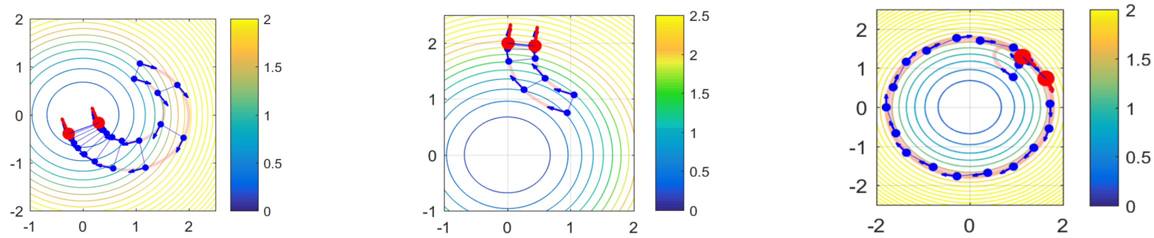

(a) $z^d = 0,\ k_2 = 0$ (b) $z^d \neq 0,\ k_2 = 0$ (c) $z^d \neq 0,\ k_2 \neq 0$

Fig. 2: The blue arrows are the velocities which turn red at the end time. The circular curves are the field level curves.

where $\boldsymbol{N}_c = \frac{\nabla z_c}{\|\nabla z_c\|}$, *and* $\hat{\nu} = \frac{k_1}{\lambda^q - \lambda^n} \sum_{k=1}^{M} \nu_k \langle \boldsymbol{r}_k - \boldsymbol{r}_c, \boldsymbol{q} \rangle$.

See proof in Section VIII.

Since $\boldsymbol{n}$ and $\boldsymbol{q}$ are orthonormal, we can write $\boldsymbol{q}\boldsymbol{q}^\intercal = \boldsymbol{I} - \boldsymbol{n}\boldsymbol{n}^\intercal$. Hence, we can reform (11) as

$$\dot{\boldsymbol{n}} = -k_1 \frac{\lambda^q}{\lambda^q - \lambda^n} \|\nabla z_c\| (\boldsymbol{I} - \boldsymbol{n}\boldsymbol{n}^\intercal) \boldsymbol{N}_c - \hat{\nu} \boldsymbol{q}. \tag{13}$$

Note that the second term in (13) vanishes when $\nu_k = \nu$ for all agents. i.e. the field is linear, or when the agents are at the same level curve.

Remark 3. *The first term in (13) represents a consensus-on-a sphere control law [26]. This is interesting since although we are explicitly applying (4) with (3), the direction* $\boldsymbol{n}$ *is implicitly tracking the negative direction of the gradient* $-\boldsymbol{N}_c$.

V. Convergence Analysis

Recall that the PCA flow (3) runs in the time scale τ, while the control law (4) runs in the time scale t. That is, for each time instance t, each agent runs (3) for some time τ. Let the relationships between the control time t, and the PCA perception time τ be $\frac{dt}{d\tau} = \epsilon$, where $\epsilon \in (0, 1)$. This implies that $\tau = \frac{t - t_0}{\epsilon}$, where $\tau_0 = 0$. Using this relationship, the perception and control dynamics in the singular perturbation framework are

$$\dot{\boldsymbol{r}}_i = k_1(z_i - z^d)\boldsymbol{n} + k_2 \boldsymbol{q}, \quad \forall i, \tag{14}$$

$$\dot{\boldsymbol{n}} = g_1(\cdot), \tag{15}$$

$$\dot{\boldsymbol{q}} = g_2(\cdot), \tag{16}$$

$$\epsilon \dot{\hat{\boldsymbol{q}}} = (\boldsymbol{I} - \hat{\boldsymbol{q}}\hat{\boldsymbol{q}}^\intercal) \boldsymbol{C} \hat{\boldsymbol{q}}. \tag{17}$$

where $g_1(\cdot)$ and $g_2(\cdot)$ are the general information dynamics equations given by (7) and (8). The control dynamics (14)-(16) are viewed as a slow system whereas the perception dynamics (17) are viewed as a fast system.

In what follows, we first obtain the conditions under which we prove that (A) the SUSD direction $\boldsymbol{n}$ converges to the negative gradient direction $-\boldsymbol{N}_c$, and the conditions under which we prove that (B) trajectories $z(\boldsymbol{r}_c) - z^d$ for level curve tracking, or of $z(\boldsymbol{r}_c)$ for source seeking, are ultimately bounded.

A. Convergence of the SUSD Direction

Define

$$\theta = 1 + \langle \boldsymbol{N}_c, \boldsymbol{n} \rangle, \tag{18}$$

where $\theta \to 0$ when $\boldsymbol{n} \to -\boldsymbol{N}_c$. i.e. when the swarm is moving in the negative direction of the field gradient. Additionally, define

$$\psi = 1 - \langle \boldsymbol{q}, \hat{\boldsymbol{q}} \rangle, \tag{19}$$

where $\psi \to 0$ when $\hat{\boldsymbol{q}} \to \boldsymbol{q}$, i.e when the PCA perception algorithm converges to the exact eigenvector of the covariance matrix $\boldsymbol{C}$. We then obtain the coerced slow and fast systems

$$\dot{\theta} = k_1 \|\nabla z_c\| \frac{\lambda^q}{\lambda^q - \lambda^n} \theta(\theta - 2) + \delta, \tag{20}$$

$$\epsilon \dot{\psi} = -(\lambda^q - \lambda^n)\psi(1 - \psi)(2 - \psi) + \epsilon \eta, \tag{21}$$

where δ is viewed as an input disturbance due to the nonlinearity of the field, and η represents the interconnection between the coerced slow and fast systems. They are defined by

$$\delta = -\frac{k_1}{\lambda^q - \lambda^n} \vartheta \langle \boldsymbol{N}_c, \boldsymbol{q} \rangle + \langle \boldsymbol{n}, \dot{\boldsymbol{N}}_c \rangle,$$
$$\eta = \pm \frac{k_1}{\lambda^q - \lambda^n} \Big(\vartheta \pm \|\nabla z_c\| \lambda^q \sqrt{\theta(2 - \theta)} \Big) \sqrt{\psi(2 - \psi)}, \tag{22}$$

where $\vartheta = \sum_{k=1}^{M} \nu_k \langle \boldsymbol{r}_k - \boldsymbol{r}_c, \boldsymbol{q} \rangle$, and $\langle \boldsymbol{n}, \dot{\boldsymbol{N}}_c \rangle = \frac{1}{\|\nabla z_c\|} \boldsymbol{n}^\intercal (\boldsymbol{I} - \boldsymbol{N}_c \boldsymbol{N}_c^\intercal) \nabla^2 z_c (k_1(z_a - z_d)\boldsymbol{n} + k_2 \boldsymbol{q})$, where z_a is the average field measurement and $\nabla^2 z_c$ is the hessian matrix of the field.

Proof. of (20) and (21). To derive (20), we take the time derivative of (18) and apply (13) of **Lemma** IV.3 for $\dot{\boldsymbol{n}}$. On the other hand, we derive (21) by the following steps. By the Chain rule, $\frac{d\hat{\boldsymbol{q}}}{d\tau} = \epsilon \frac{d\hat{\boldsymbol{q}}}{dt}$, or $\frac{d\hat{\boldsymbol{q}}}{dt} = \frac{1}{\epsilon} \frac{d\hat{\boldsymbol{q}}}{d\tau}$. Hence

$$\frac{d\psi}{d\tau} = \epsilon \frac{d\psi}{dt} = -\epsilon \langle \frac{d\boldsymbol{q}}{dt}, \hat{\boldsymbol{q}} \rangle - \langle \boldsymbol{q}, \frac{d\hat{\boldsymbol{q}}}{d\tau} \rangle. \tag{23}$$

From (3), we obtain

$$\langle \boldsymbol{q}, \frac{d\hat{\boldsymbol{q}}}{d\tau} \rangle = (1 - \psi) \Big(\lambda^q - \langle \hat{\boldsymbol{q}}, \boldsymbol{C} \hat{\boldsymbol{q}} \rangle \Big). \tag{24}$$

Write $\hat{\boldsymbol{q}} = \langle \hat{\boldsymbol{q}}, \boldsymbol{q} \rangle \boldsymbol{q} + \langle \hat{\boldsymbol{q}}, \boldsymbol{n} \rangle \boldsymbol{n}$. Hence

$$\langle \hat{\boldsymbol{q}}, \boldsymbol{C} \hat{\boldsymbol{q}} \rangle = \lambda^q (1 - \psi)^2 + \lambda^n \psi (2 - \psi). \tag{25}$$

Substituting (25) into (24) yields

$$\langle \boldsymbol{q}, \frac{d\hat{\boldsymbol{q}}}{d\tau} \rangle = (\lambda^q - \lambda^n) \psi (1 - \psi)(2 - \psi). \tag{26}$$

On the other hand, using (12), we obtain

$$\langle \frac{d\boldsymbol{q}}{dt}, \hat{\boldsymbol{q}} \rangle = \frac{k_1}{\lambda^q - \lambda^n} \Big(\|\nabla z_c\| \lambda^q \langle \boldsymbol{N}_c, \boldsymbol{q} \rangle + \vartheta \Big) \langle \boldsymbol{n}, \hat{\boldsymbol{q}} \rangle, \tag{27}$$

where $\vartheta = \sum_{k=1}^{M} \nu_k \langle \boldsymbol{r}_k - \boldsymbol{r}_c, \boldsymbol{q} \rangle$, and $\langle \boldsymbol{n}, \hat{\boldsymbol{q}} \rangle = \pm\sqrt{\psi(2-\psi)}$. Substituting (26) and (27) in (23), we obtain

$$\frac{d\psi}{d\tau} = \epsilon \frac{d\psi}{dt} = -(\lambda^q - \lambda^n)\psi(1-\psi)(2-\psi) + \epsilon\eta, \quad (28)$$

where η is as defined by (22). □

We first let $\epsilon = 0$ in (20) and (21) to analyze the stability of the resulting decoupled reduced and boundary systems (29) and (34), respectively. Then, we analyze the stability of the coupled system of (20) and (21) by deriving $\epsilon^* \in (0,1)$ such that for all $\epsilon \leq \epsilon^*$, some of the stability results of the reduced and boundary systems, (29) and (34), hold for the coupled system.

1) Stability of the Reduced System: The coerced reduced system is given by

$$\dot{\theta} = -k_1 \|\nabla z_c\| \frac{\lambda^q}{\lambda^q - \lambda^n} \theta(2-\theta) + \delta = f(t, \theta, \delta). \quad (29)$$

Note that, when $\theta \in \{0, 2\}$, then $\boldsymbol{n} = \pm \boldsymbol{N}_c$ which implies that $\langle \boldsymbol{N}_c, \boldsymbol{q} \rangle = 0$ and $\boldsymbol{n}^\intercal(\boldsymbol{I} - \boldsymbol{N}_c \boldsymbol{N}_c^\intercal) = 0$. Hence δ vanishes at the equilibria $\theta \in \{0, 2\}$. Additionally observe that $\delta = 0$ when $\nabla^2 z_c = 0$ and $\nu_k = 0$, $\forall k$, i.e. when the field is linear.

The following result describes the stability of the origin of the reduced system.

Theorem V.1. *Consider the reduced system (29). Suppose there exists a lower bound $\mu_1 > 0$ such that $\|\nabla z(\boldsymbol{r}_c)\| > \mu_1$. Then the equilibrium $\theta = 0$ of the unforced system $f(t, \theta, 0)$ is asymptotically stable in which whenever $\theta(0) \in [0, 2)$, then $\theta(t) \to 0$ as $t \to \infty$. Furthermore, for an input disturbance satisfying $|\delta| \leq k_1 \epsilon_1 \frac{\lambda^q}{\lambda^q - \lambda^n} \mu_1$, where $\epsilon_1 \in (0,1)$, the equilibrium $\theta = 0$ of forced system $f(t, \theta, \delta)$ is locally input-to-state stable.*

Proof. Consider the domain $\boldsymbol{D}_1 = \{\theta | \theta \in [0, 2)\}$ i.e. $\langle \boldsymbol{N}_c, \boldsymbol{n} \rangle \neq 1$. Let $V_1 : \boldsymbol{D}_1 \to \boldsymbol{R}$ be a Lyapunov candidate function defined by

$$V_1 = \frac{\theta}{2 - \theta}, \quad (30)$$

where $V_1 = 0$ if and only if $\theta = 0$. Additionally, $V_1 \to \infty$ as $\theta \to 2$. For the unforced system $f(t, \theta, 0)$, we obtain

$$\dot{V}_1 = -2k_1 \|\nabla z_c\| \frac{\lambda^q}{\lambda^q - \lambda^n} V_1 \leq 0. \quad (31)$$

Since $\dot{V}_1 = 0$ if and only if $\theta = 0$, then the origin of the unforced system $f(t, \theta, 0)$ is asymptotically stable. Additionally, $\dot{V}_1 \to -\infty$ as $\theta \to 2$. This along with the fact that $V_1 \to \infty$ whenever $\theta \to 2$ and $\|\nabla z_c\| > \mu_1 > 0$, implies that $\boldsymbol{D}_1$ is a forward invariant set, and thus $\theta \in [0, 2)$ for all t.

For the forced system $f(t, \theta, \delta)$, we obtain

$$\dot{V}_1 \leq -2(1 - \epsilon_1) k_1 \mu_1 \frac{\lambda^q}{\lambda^q - \lambda^n} V_1, \quad \forall |\theta| \geq \rho(|\delta|), \quad (32)$$

where $\rho(|\delta|) = 1 - \sqrt{1 - \frac{(\lambda^q - \lambda^n)|\delta|}{k_1 \epsilon_1 \lambda^q \mu_1}}$ is a class $\mathcal{K}$ function in the domain $[0, k_1 \epsilon_1 \frac{\lambda^q}{\lambda^q - \lambda^n} \mu_1]$. Let $\alpha_1(|\theta|) = \alpha_2(|\theta|) = \frac{|\theta|}{2 - |\theta|}$ which are class $\mathcal{K}$ functions that satisfy: $\alpha_1(|\theta|) \leq V_1(\theta) \leq \alpha_2(|\theta|)$[1]. Therefore, using **Definition 3.3** of local input-to-state stability in [14], and according to **Theorem 4.19** in [19], the origin of the forced system $f(t, \theta, \delta)$ is locally input-to-state stable. □

Remark 4. *In **Theorem V.1** we showed that the set $\{\theta | \theta \in [0, 2)\}$ is forward invariant. By If we modify V_1 in (30) to be $V_1 = \frac{2\theta}{1 - \theta}$, where $V_1 : [0, 1) \to \boldsymbol{R}$, then we can show that $\dot{V}_1$ satisfies (32). Hence, using the same argument in proving **Theorem V.1**, we can show that the set $\{\theta | \theta \in [0, 1)\}$ is also forward invariant.*

Lemma V.2. *The assumption in Theorem V.1 that the input disturbance satisfies $|\delta| \leq k_1 \epsilon_1 \frac{\lambda^q}{\lambda^q - \lambda^n} \mu_1$ is valid whenever $\|\nabla z(\boldsymbol{r}_c)\| > \mu_1$ where*

$$\mu_1 = \frac{|\vartheta| + \sqrt{|\vartheta|^2 + 4\epsilon_1 \lambda^q (\lambda^q - \lambda^n)(|z_a - z_d| + \frac{k_2}{k_1}) \|\nabla^2 z_c\|}}{2\epsilon_1 \lambda^q}, \quad (33)$$

in which ϑ is as defined in (22). See proof in Section VIII.

Observe that **Theorem V.1** implies that wherever the swarm is in a landscape where $\|\nabla z(\boldsymbol{r}_c)\| > \mu_1$, then the SUSD direction $\boldsymbol{n}$ follows the negative gradient direction $-\boldsymbol{N}$. Since according to **Assumption II.3** the field has a unique minimum, then the bound μ_1 defines a neighborhood around the source location $\boldsymbol{r}_0$ where the magnitude of the gradient $\|\nabla z(\boldsymbol{r}_c)\|$ is dominated by the higher-order terms.

2) Stability of the Boundary System: By setting $\epsilon = 0$ in (28), we obtain the boundary system

$$\frac{d\psi}{d\tau} = -(\lambda^q - \lambda^n)\psi(1-\psi)(2-\psi). \quad (34)$$

Observe that in (34), λ^q and λ^n are constants with respect to the time scale τ. Additionally, system (34) is at equilibrium when $\psi \in \{0, 1, 2\}$. The desired equilibrium $\psi = 0$ corresponds to $\hat{\boldsymbol{q}} = \boldsymbol{q}$, and the undesired $\psi = 1$ and $\psi = 2$ correspond to $\hat{\boldsymbol{q}} = \pm \boldsymbol{n}$ and $\hat{\boldsymbol{q}} = -\boldsymbol{q}$, respectively. We have the following result for origin of the boundary system

Theorem V.3. *The origin of the boundary system (34) is asymptotically stable uniformly in λ^q and λ^n, in which whenever at $\tau = 0$, $\psi(0) \in [0, 1)$, then $\psi \to 0$ as $\tau \to \infty$.*

Proof. Let $\boldsymbol{D}_2 = \{\psi \in \mathbb{R} | \psi \in [0, 1)\}$ which is equivalent to $0 < \langle \boldsymbol{q}, \hat{\boldsymbol{q}} \rangle \leq 1$. Then let $V_2(\psi) : \boldsymbol{D}_2 \to \mathbb{R}$ be a Lyapunov candidate function defined by

$$V_2 = \frac{\psi}{1 - \psi} \quad (35)$$

where $V_2 \geq 0$ and $V_2 = 0$ if and only if $\psi = 0$. Furthermore, $V_2 \to \infty$ as $\psi \to 1$. Using (34), we obtain

$$\frac{dV_2}{d\tau} = -(\lambda^q - \lambda^n)(2 - \psi) V_2 \leq 0, \quad (36)$$

where in $\boldsymbol{D}_2$, $\frac{dV_2}{d\tau} = 0$ if and only if $\psi = 0$. Furthermore, since from **Assumption** III.1 $(\lambda^q - \lambda^n) \neq 0$, then $\frac{dV_2}{d\tau} \to -\infty$ as $\psi \to 1$. This along with the fact that $V_2 \to \infty$ whenever

[1]For more details about the definitions of class $\mathcal{K}$ functions, the reader is referred to **Definition 4.2** of [19].

$\psi \to 1$ implies that $\boldsymbol{D}_2$ is a forward invariant set, and thus $\psi(\tau) \in [0, 1)$ for all τ. Let $W_1(\psi) = W_2(\psi) = V_2$ which implies that $W_1(\psi) \leq V_2 \leq W_2(\psi)$. Consequently, according to **Theorem 4.9** in [19], we can conclude that the equilibrium $\psi = 0$ of the boundary system (34) is asymptotically stable, uniformly in λ^q and λ^n. □

3) Stability of the Unforced Coupled System: Substituting for $\delta = 0$ in (20) and (21), we obtain the unforced coupled system

$$\dot{\theta} = k_1 \|\nabla z_c\| \frac{\lambda^q}{\lambda^q - \lambda^n} \theta(\theta - 2) \triangleq f(t, \theta(t), 0, 0), \tag{37}$$

$$\epsilon\dot{\psi} = -(\lambda^q - \lambda^n)\psi(1 - \psi)(2 - \psi) + \epsilon\eta \triangleq g(t, \theta(t), \psi(t), \epsilon), \tag{38}$$

where $\eta = \pm k_1 \|\nabla z_c\| \frac{\lambda^q}{\lambda^q - \lambda^n} \sqrt{\theta(2 - \theta)}\sqrt{\psi(2 - \psi)}$.

Theorem V.4. *Consider the coupled system given by (37) and (38). Assume that $0 < \mu_1 \leq \|\nabla z_c\| \leq \mu_2 < \infty$ and $0 < \chi_1 \leq \lambda^q - \lambda^n \leq \chi_2 < \infty$ where μ_1, μ_2, χ_1 and χ_2 are constants. Furthermore, assume that $\epsilon < \epsilon_d$ where*

$$\epsilon_d = \frac{2(1 - d)\mu_1 \chi_1^3}{d k_1 \mu_2^2 \chi_2^2}, \tag{39}$$

in which $d \in (0, 1)$ is a constant. Then the origin $(\theta, \psi) = (0, 0)$ is uniformly asymptotically stable in which whenever $\theta(0) \in [0, 2)$ and $\psi(0) \in [0, 1)$, then $(\theta(t), \psi(t)) \to (0, 0)$ as $t \to \infty$.

Proof. Consider $(t, \theta, \psi, \epsilon) \in [t_0, \infty) \times [0, 2) \times [0, 1) \times [0, \epsilon_0]$. Then, the origin $(\theta, \psi) = (0, 0)$ is the unique equilibrium of $0 = f(t, 0, 0, \epsilon)$ and $0 = g(t, 0, 0, \epsilon)$. Moreover, $0 = g(t, \theta, \psi, 0)$ has a unique root $z = h(t, \theta) = 0$.

In the proof of **Theorem** V.1, we showed that the positive definite $V_1(t, \theta) = \frac{\theta}{2-\theta}$ satisfies (i): $\alpha_1(|\theta|) \leq V_1(t, \theta) \leq \alpha_2(|\theta|)$ where $\alpha_1(|\theta|) = \alpha_2(|\theta|) = \frac{|\theta|}{2-|\theta|}$ are class $\mathcal{K}$ functions, and, since $\|\nabla z_c\| \geq \mu_1$ and $\frac{\lambda^q}{\lambda^q - \lambda^n} \geq 1$, (ii): $\frac{\partial V_1}{\partial t} + \frac{\partial V_1}{\partial \theta} f(t, \theta, 0, 0) \leq -\varrho_1 U_1^2(\theta)$ where $\varrho_1 = 2k_1\mu_1$ is a constant, and $U_1(\theta) = \sqrt{\frac{\theta}{2-\theta}}$ is a continuous scalar function that vanishes only when $\theta = 0$.

Similarly, in the proof of **Theorem** V.3, we showed that the positive definite $V_2(t, \psi) = \frac{\psi}{1-\psi}$ satisfies (iii) $W_1(\psi) \leq V_2(t, \psi) \leq W_2(\psi)$ where $W_1(\psi) = W_2(\psi) = \frac{\psi}{1-\psi}$ are class $\mathcal{K}$ functions, and, since $(\lambda^q - \lambda^n) \geq \chi_1$, (iv): $\frac{\partial V_2}{\partial \psi} g(t, \theta, \psi, 0) \leq -\varrho_2 U_2^2(\psi)$, where $\varrho_2 = \chi_1$ and $U_2(\psi) = \sqrt{\frac{\psi(2-\psi)}{1-\psi}}$ is a continuous scalar function that vanishes only when $\psi = 0$.

For the interconnected system, we have (v): $\frac{\partial V_1}{\partial \theta}[f(t, \theta, \psi, \epsilon) - f(t, \theta, h(t, x), 0)] = \frac{\partial V}{\partial \theta}[f(t, \theta, 0, 0) - f(t, \theta, 0, 0)] = 0$ where we used the fact that f is independent of ψ and ϵ. Similarly, since V_2 does explicitly depend on t and θ, we have (vi): $\frac{\partial V_2}{\partial t} + \frac{\partial V_2}{\partial \theta} f(t, \theta, \psi, \epsilon) = 0$. Finally, we derive (vii): $\frac{\partial V_2}{\partial \psi}[g(t, \theta, \psi, \epsilon) - g(t, \theta, \psi, 0)] = \epsilon\eta \leq \epsilon\varrho_3 U_1(\theta) U_2(\psi)$, where $\varrho_3 = 2k_1\mu_2\frac{\chi_2}{\chi_1}$.

Through (i) to (vii), we satisfy all the assumptions required by **Theorem 5.1** in [23]. Hence, according to **Theorem 5.1** in [23], for every $d \in (0, 1)$, $v(t, \theta, \psi) = (1 - d)V_1(t, \theta) + dV_2(t, \psi)$ is a Lyapunov function for all $\epsilon < \epsilon_d$ where ϵ_d is given by[2] (39). This implies that the origin $(\theta, \psi) = (0, 0)$ is a uniformly asymptotically stable equilibrium of the singularly perturbed system given by (37) and (38) for all $\epsilon \in (0, \epsilon_d)$. □

B. Convergence of the Swarm Trajectory

In this section, we study the convergence of the swarm to either the source location or the desired level curve. Define $z_c^d = z_c - z^d$. This implies that $z_c^d = 0$ if and only if $z_c = z^d$. Taking the time derivative, $\dot{z}_c^d = \dot{z}_c = \langle \nabla z_c, \dot{\boldsymbol{r}}_c \rangle$. But, using (14), $\dot{\boldsymbol{r}}_c = \frac{1}{M}\sum_k [k_1(z_k - z^d)\boldsymbol{n} + k_2\boldsymbol{q}] = k_1(z_a - z^d)\boldsymbol{n} + k_2\boldsymbol{q}$ where $z_a = \frac{1}{M}\sum_k z_k$ is the average field measurement. Note that , using (10), $z_a = \frac{1}{M}\sum_k z_k = \frac{1}{M}\sum_{k=1}^M [z_c + \langle \nabla z_c, \boldsymbol{r}_k - \boldsymbol{r}_c \rangle + \nu_k] = z_c + \nu$ where $\nu = \frac{1}{M}\sum_{k=1}^M \nu_k$ and $\frac{1}{M}\sum_{k=1}^M \langle \nabla z_c, \boldsymbol{r}_k - \boldsymbol{r}_c \rangle = 0$. That is the difference between the average and center measurements equals to the average of higher-order terms. Then we obtain

$$\dot{z}_c^d = k_1\|\nabla z_c\|(z_c^d + \nu)\langle \boldsymbol{N}, \boldsymbol{n} \rangle + k_2\|\nabla z_c\|\langle \boldsymbol{N}, \boldsymbol{q} \rangle, \tag{40}$$

where $\nu = z_a - z_c$. Note that, even when $\langle \boldsymbol{N}, \boldsymbol{n} \rangle = \pm 1$ which implies $\langle \boldsymbol{N}, \boldsymbol{q} \rangle = 0$, $z_c^d = 0$ is not an equilibrium to (40) due to the existence of ν. In the following, we present a boundedness result for the trajectory $z_c^d(t)$.

Theorem V.5. *Suppose $\|\nabla z(\boldsymbol{r}_c)\| > \mu_3$ where $\mu_3 > 0$ is a constant. Furthermore, suppose $-1 \leq \langle \boldsymbol{N}, \boldsymbol{n} \rangle \leq -\epsilon_2$ and $|\nu| \leq \bar{\nu}$, where $\epsilon_2 \in (0, 1)$ and $\bar{\nu} > 0$ are constants. Then, the solutions of (40) are uniformly ultimately bounded.*

Proof. Let $V_3 : \boldsymbol{R} \to \boldsymbol{R}$ be a Lyapunov candidate function defined by $V_3 = \frac{1}{2}(z_c^d)^2$, where $V_3 = 0$ if and only if $z_c^d = 0$. Then we obtain

$$\dot{V}_3 \leq -2k_1\mu_3\epsilon_2(1 - \epsilon_2)V_3, \forall |z_c^d| \geq \frac{k_1\bar{\nu} + k_2\sqrt{1 - \epsilon_2^2}}{k_1\epsilon_2^2}, \tag{41}$$

where $\dot{V}_3 = 0$ if and only if $z_c^d = 0$. Let $\alpha_3(|z_c^d|) = \alpha_4(|z_c^d|) = \frac{1}{2}|z_c^d|^2$ be class $\mathcal{K}$ functions. Then $\alpha_3(|z_c^d|) \leq V_3 \leq \alpha_4(|z_c^d|)$. Therefore, according to **Theorem 4.18** in [19], the trajectories of the system (40) are uniformly ultimately bounded. □

Note that we proved in **Remark** 4 that the required assumption $-1 \leq \langle \boldsymbol{N}, \boldsymbol{n} \rangle \leq -\epsilon_2 < 0$ can be satisfied. Further, note that, (41) implies that the z_c^d trajectories of (40) will converge to a strip around the desired level curve and the strip is defined by $\{\boldsymbol{r}_c | |z_c^d| \leq \frac{k_1\bar{\nu} + k_2\sqrt{1-\epsilon_2^2}}{k_1\epsilon_2^2}\}$. If we only consider source seeking, i.e. $k_2 = 0$ and $z_c^d = z_c$, then the z_c trajectories of (40) will converge to a neighborhood around the source location defined by $\{\boldsymbol{r}_c | |z_c^d| \leq \frac{\bar{\nu}}{\epsilon_2^2}\}$.

VI. Experimental Results

In [1], [3], we presented several simulation results. Here we validate the model through experiments. In the first experiment, we used the Georgia Tech Miniature Blimps [11] with light sensors to perform source seeking in a physical light field. The diameter of each blimp is about 0.7 m and the dimensions of the experimental space are about 4 m ×

[2] We derived ϵ_d by using (5.12) in [23] using all the corresponding coefficients derived in (i) through (vii).

This article has been accepted for publication in a future issue of this journal, but has not been fully edited. Content may change prior to final publication. Citation information: DOI 10.1109/TAC.2021.3077457, IEEE Transactions on Automatic Control

4 m. To make the minimum at the source, we inverted the field by using $\frac{1}{z_i}$ instead of z_i. We set $\epsilon = 0.01$, $k_1 = 1$, $k_2 = 0$ and $z^d = 0$ in (17). Snapshots of the experiment are shown in Fig. 3. Despite that initially $\langle \boldsymbol{N}, \boldsymbol{n} \rangle > 0$ and the potential noisy measurements, the two blimps are able to find the source.

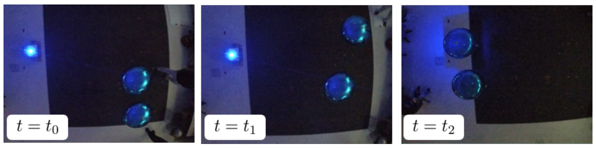

Fig. 3: The two blimps initially have $\langle \boldsymbol{N}, \boldsymbol{n} \rangle > 0$.

For the second experiment, we implemented the level curve tracking using four mobile robots at the Robotarium [30]. We used a virtual nonconvex field with mathematical expression given in [1]. We set $z^d = 2$, $\epsilon = 0.01$, $k_1 = 2$, and $k_2 = 0.5$. In Fig. 4 we present the trajectories of the robot. Despite the graph is incomplete, the swarm is able to track the desired level curve smoothly.

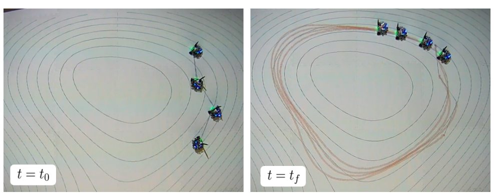

Fig. 4: Four robots in a nonconvex field.

VII. Conclusion

In this paper, we proposed a distributed active perception strategy for source seeking and level curve tracking without the need to explicitly estimate the field gradient or explicitly share measurements among the agents. We obtained several stability results in a singular perturbation framework justifying the robustness and convergence of the algorithms. The simulation and experimental results suggest the efficiency of the proposed model. In the future, we consider the incomplete graph case. Additionally, we will design control laws for different swarm applications within the proposed framework of distributed active perception.

ACKNOWLEDGEMENTS

S. Al-Abri and F. Zhang were supported by ONR grants N00014-19-1-2556 and N00014-19-1-2266; NSF grants OCE-1559475, CNS-1828678, and S&AS-1849228; NRL grants N00173-17-1-G001 and N00173-19-P-1412 ; and NOAA grant NA16NOS0120028.

VIII. Proofs of the information dynamics

Proof of Lemma IV.1. The covariance matrix satisfies $\boldsymbol{C}\boldsymbol{n} = \lambda^n \boldsymbol{n}$, and $\boldsymbol{C}\boldsymbol{q} = \lambda^q \boldsymbol{q}$. Since with Assumption III.1, the eigenvalues and eigenvectors of $\boldsymbol{C}$ are uniquely defined, then their derivatives exist. Thus, taking the derivative, we obtain

$$\dot{\boldsymbol{C}}\boldsymbol{n} + \boldsymbol{C}\dot{\boldsymbol{n}} = \dot{\lambda}^n \boldsymbol{n} + \lambda^n \dot{\boldsymbol{n}}, \tag{42}$$

$$\dot{\boldsymbol{C}}\boldsymbol{q} + \boldsymbol{C}\dot{\boldsymbol{q}} = \dot{\lambda}^q \boldsymbol{q} + \lambda^q \dot{\boldsymbol{q}}. \tag{43}$$

Inner product both sides of (42) with the eigenvector $\boldsymbol{q}$, and both sides of (43) with the eigenvector $\boldsymbol{n}$

$$\langle \boldsymbol{q}, \dot{\boldsymbol{C}}\boldsymbol{n} \rangle + \langle \boldsymbol{q}, \boldsymbol{C}\dot{\boldsymbol{n}} \rangle = \dot{\lambda}^n \langle \boldsymbol{q}, \boldsymbol{n} \rangle + \lambda^n \langle \boldsymbol{q}, \dot{\boldsymbol{n}} \rangle, \tag{44}$$

$$\langle \boldsymbol{n}, \dot{\boldsymbol{C}}\boldsymbol{q} \rangle + \langle \boldsymbol{n}, \boldsymbol{C}\dot{\boldsymbol{q}} \rangle = \dot{\lambda}^q \langle \boldsymbol{n}, \boldsymbol{q} \rangle + \lambda^q \langle \boldsymbol{n}, \dot{\boldsymbol{q}} \rangle. \tag{45}$$

Since $\boldsymbol{C}$ is symmetric, then $\dot{\boldsymbol{C}}$ is also symmetric. This implies that $\langle \boldsymbol{q}, \boldsymbol{C}\dot{\boldsymbol{n}} \rangle = \langle \boldsymbol{C}\boldsymbol{q}, \dot{\boldsymbol{n}} \rangle = \lambda^q \langle \boldsymbol{q}, \dot{\boldsymbol{n}} \rangle$. Similarly, $\langle \boldsymbol{n}, \boldsymbol{C}\dot{\boldsymbol{q}} \rangle = \langle \boldsymbol{C}\boldsymbol{n}, \dot{\boldsymbol{q}} \rangle = \lambda^n \langle \boldsymbol{n}, \dot{\boldsymbol{q}} \rangle$. Using these along with the fact that $\langle \boldsymbol{q}, \boldsymbol{n} \rangle = \langle \boldsymbol{n}, \boldsymbol{q} \rangle = 0$, we obtain from (44) and (45)

$$\langle \boldsymbol{q}, \dot{\boldsymbol{n}} \rangle = -\frac{1}{\lambda^q - \lambda^n} \langle \boldsymbol{q}, \dot{\boldsymbol{C}}\boldsymbol{n} \rangle, \tag{46}$$

$$\langle \boldsymbol{n}, \dot{\boldsymbol{q}} \rangle = \frac{1}{\lambda^q - \lambda^n} \langle \boldsymbol{q}, \dot{\boldsymbol{C}}\boldsymbol{n} \rangle. \tag{47}$$

Since $\boldsymbol{n}$ and $\boldsymbol{q}$ are orthonormal, then we can write

$$\dot{\boldsymbol{n}} = \langle \boldsymbol{q}, \dot{\boldsymbol{n}} \rangle \boldsymbol{q}, \quad \dot{\boldsymbol{q}} = \langle \boldsymbol{n}, \dot{\boldsymbol{q}} \rangle \boldsymbol{n}. \tag{48}$$

Substituting (46) and (47) in (48)

$$\dot{\boldsymbol{n}} = -\frac{1}{\lambda^q - \lambda^n} \langle \boldsymbol{q}, \dot{\boldsymbol{C}}\boldsymbol{n} \rangle \boldsymbol{q} \tag{49}$$

$$\dot{\boldsymbol{q}} = \frac{1}{\lambda^q - \lambda^n} \langle \boldsymbol{q}, \dot{\boldsymbol{C}}\boldsymbol{n} \rangle \boldsymbol{n}. \tag{50}$$

Taking the derivative of the covariance (2), we obtain

$$\dot{\boldsymbol{C}} = \sum_{k=1}^{M} [(\dot{\boldsymbol{r}}_k - \dot{\boldsymbol{r}}_c)(\boldsymbol{r}_k - \boldsymbol{r}_c)^\mathsf{T} + (\boldsymbol{r}_k - \boldsymbol{r}_c)(\dot{\boldsymbol{r}}_k - \dot{\boldsymbol{r}}_c)^\mathsf{T}]. \tag{51}$$

But using (1)

$$\dot{\boldsymbol{r}}_k - \dot{\boldsymbol{r}}_c = \boldsymbol{u}_k - \frac{1}{M}\sum_{l=1}^{M} \boldsymbol{u}_l = \frac{1}{M}\sum_{l=1}^{M} (\boldsymbol{u}_k - \boldsymbol{u}_l). \tag{52}$$

Hence, substituting (52) in (51)

$$\begin{aligned}\dot{\boldsymbol{C}} &= \frac{1}{M}\sum_{k=1}^{M}\sum_{l=1}^{M} (\boldsymbol{u}_k - \boldsymbol{u}_l)(\boldsymbol{r}_k - \boldsymbol{r}_c)^\mathsf{T} \\ &+ \frac{1}{M}\sum_{k=1}^{M} (\boldsymbol{r}_k - \boldsymbol{r}_c) \sum_{l=1}^{M} (\boldsymbol{u}_k - \boldsymbol{u}_l)^\mathsf{T} \\ &= \sum_{k=1}^{M} \left[\boldsymbol{u}_k (\boldsymbol{r}_k - \boldsymbol{r}_c)^\mathsf{T} + (\boldsymbol{r}_k - \boldsymbol{r}_c)\boldsymbol{u}_k^\mathsf{T}\right]. \end{aligned} \tag{53}$$

Finally, substituting (53) in (49) and (50) leads to the desired result (6). □

Proof of Lemma IV.2. Substituting the control law (4) in (53), using the fact that $\sum_{k=1}^{M} (\boldsymbol{r}_k - \boldsymbol{r}_c) = 0$, we obtain

$$\dot{\boldsymbol{C}} = \sum_{k=1}^{M} k_1 (z_k^d - z_c^d) \Big[\boldsymbol{n}(\boldsymbol{r}_k - \boldsymbol{r}_c)^\mathsf{T} + (\boldsymbol{r}_k - \boldsymbol{r}_c)\boldsymbol{n}^\mathsf{T}\Big], \tag{54}$$

where $z_k^d = z_k - z^d$ and $z_c^d = z_c - z^d$. We then derive

$$\langle \boldsymbol{n}, \dot{\boldsymbol{C}}\boldsymbol{q} \rangle = k_1 \sum_{k=1}^{M} (z_k^d - z_c^d) \langle \boldsymbol{r}_k - \boldsymbol{r}_c, \boldsymbol{q} \rangle. \tag{55}$$

Finally, since $z_k^d - z_c^d = z_k - z^d - (z_c - z^d) = z_k - z_c$, we obtain (7) and (8) by substituting (55) in (49) and (50), respectively.

□

Proof of Lemma IV.3. Substituting $(z_k - z_c)$ from (10) into (9) yields

$$\boldsymbol{w} = \sum_{k=1}^{M} [\langle \boldsymbol{r}_k - \boldsymbol{r}_c, \nabla z_c \rangle (\boldsymbol{r}_k - \boldsymbol{r}_c) + \nu_k (\boldsymbol{r}_k - \boldsymbol{r}_c)]. \quad (56)$$

But, $\sum_{k=1}^{M} \langle \boldsymbol{r}_k - \boldsymbol{r}_c, \boldsymbol{\nabla z_c} \rangle (\boldsymbol{r}_k - \boldsymbol{r}_c) = \sum_{k=1}^{M} (\boldsymbol{r}_k - \boldsymbol{r}_c)(\boldsymbol{r}_k - \boldsymbol{r}_c)^\intercal \nabla z_c = \boldsymbol{C} \nabla z_c$. Hence

$$\boldsymbol{w} = \boldsymbol{C} \nabla z_c + \sum_{k=1}^{M} \nu_k (\boldsymbol{r}_k - \boldsymbol{r}_c). \quad (57)$$

Finally, using $\hat{\nu} = \frac{k_1}{\lambda^q - \lambda^n} \sum_{k=1}^{M} \nu_k \langle \boldsymbol{r}_k - \boldsymbol{r}_c, \boldsymbol{q} \rangle$, and substituting (57) in (7) and (8) yields the claimed (11) and (12). □

Proof of Lemma V.2. In order for $\rho(|\delta|)$ to be a real number, we must have $\sqrt{1 - \frac{(\lambda^q - \lambda^n)|\delta|}{k_1 \epsilon_1 \lambda^q \mu_1}} \geq 0$ which implies that $\|\nabla z_c\| > \mu_1 \geq \frac{(\lambda^q - \lambda^n)|\delta|}{k_1 \epsilon_1 \lambda^q}$. But $|\delta| \leq |\delta_1| + |\delta_2| \leq \frac{k_1}{\lambda^q - \lambda^n} |\vartheta| + \frac{k_1 |z_a - z_d| + k_2}{\|\nabla z_c\|} \|\nabla^2 z_c\|$, where $\vartheta = \sum_k \nu_k \langle \boldsymbol{r}_k - \boldsymbol{r}_c, \boldsymbol{q} \rangle$ and $\nabla^2 z_c$ is the Hessian matrix. Then we must have $\|\nabla z_c\| > \frac{1}{\epsilon_1 \lambda^q} |\vartheta| + \frac{(\lambda^q - \lambda^n)(k_1 |z_a - z_d| + k_2)}{k_1 \epsilon_1 \lambda^q \|\nabla z_c\|} \|\nabla^2 z_c\|$. Solving this inequality yields the desired result (33). □

References

[1] Said Al-Abri, Sean Maxon, and Fumin Zhang. Integrating a PCA learning algorithm with the SUSD strategy for a collective source seeking behavior. In *2018 Annual American Control Conference (ACC)*, pages 2479–2484. IEEE, 2018.

[2] Said Al-Abri, Wencen Wu, and Fumin Zhang. A gradient-free three-dimensional source seeking strategy with robustness analysis. *IEEE Transactions on Automatic Control*, 64(8):3439–3446, 2018.

[3] Said Al-Abri and Fumin Zhang. A distributed level curve tracking control law for multi-agent systems. In *2018 IEEE Conference on Decision and Control (CDC)*, pages 2575–2580. IEEE, 2018.

[4] Said Al-Abri and Fumin Zhang. A distributed active perception strategy for source seeking and level curve tracking. *arXiv preprint arXiv:2102.01856*, 2021.

[5] Pierre F Baldi and Kurt Hornik. Learning in linear neural networks: A survey. *IEEE Transactions on neural networks*, 6(4):837–858, 1995.

[6] Siavash Ahmadi Barogh and Herbert Werner. Cooperative source seeking with distance-based formation control and single-integrator agents. *IFAC-PapersOnLine*, 50(1):7911–7916, 2017.

[7] Andrew Berdahl, Colin J Torney, Christos C Ioannou, Jolyon J Faria, and Iain D Couzin. Emergent sensing of complex environments by mobile animal groups. *Science*, 339(6119):574–576, 2013.

[8] Lara Briñón-Arranz, Luca Schenato, and Alexandre Seuret. Distributed source seeking via a circular formation of agents under communication constraints. *IEEE Transactions on Control of Network Systems*, 3(2):104–115, 2015.

[9] Sarthak Chatterjee and Wencen Wu. Cooperative curve tracking in two dimensions without explicit estimation of the field gradient. In *2017 4th International Conference on Control, Decision and Information Technologies (CoDIT)*, pages 0167–0172. IEEE, 2017.

[10] Sarthak Chatterjee and Wencen Wu. A modular approach to level curve tracking with two nonholonomic mobile robots. In *International Design Engineering Technical Conferences and Computers and Information in Engineering Conference*, volume 59292, page V009T12A051. American Society of Mechanical Engineers, 2019.

[11] Sungjin Cho, Vivek Mishra, Qiuyang Tao, Paul Vamell, Matt King-Smith, Aneri Muni, Weston Smallwood, and Fumin Zhang. Autopilot design for a class of miniature autonomous blimps. In *2017 IEEE Conference on Control Technology and Applications (CCTA)*, pages 841–846. IEEE, 2017.

[12] Jennie Cochran and Miroslav Krstic. Nonholonomic source seeking with tuning of angular velocity. *IEEE Transactions on Automatic Control*, 54(4):717–731, 2009.

[13] Jennie Cochran, Antranik Siranosian, Nima Ghods, and Miroslav Krstic. 3-d source seeking for underactuated vehicles without position measurement. *IEEE Transactions on Robotics*, 25(1):117–129, 2009.

[14] SN Dashkovskiy, Denis V Efimov, and Eduardo D Sontag. Input to state stability and allied system properties. *Automation and Remote Control*, 72(8):1579, 2011.

[15] Ruggero Fabbiano, Federica Garin, and Carlos Canudas-de Wit. Distributed source seeking without global position information. *IEEE transactions on control of network systems*, 5(1):228–238, 2016.

[16] Shagun Gupta and Vipan Kakkar. Development of environmental biosensors for detection, monitoring, and assessment. In *Nanomaterials and Environmental Biotechnology*, pages 107–125. Springer, 2020.

[17] Michael Hutchinson, Hyondong Oh, and Wen-Hua Chen. A review of source term estimation methods for atmospheric dispersion events using static or mobile sensors. *Information Fusion*, 36:130–148, 2017.

[18] I. T. Jollifi. *Principal Component Analysis*. Springer, 2002.

[19] Hassan K Khalil. *Nonlinear systems*. Prentice-Hall, 2002.

[20] Alexander Khapalov. Source localization and sensor placement in environmental monitoring. *International Journal of Applied Mathematics and Computer Science*, 20(3):445–458, 2010.

[21] Sei Zhen Khong, Ying Tan, Chris Manzie, and Dragan Nešić. Multi-agent source seeking via discrete-time extremum seeking control. *Automatica*, 50(9):2312–2320, 2014.

[22] James C Kinsey, Ryan M Eustice, and Louis L Whitcomb. A survey of underwater vehicle navigation: Recent advances and new challenges. In *IFAC Conference of Manoeuvering and Control of Marine Craft*, volume 88, pages 1–12. Lisbon, 2006.

[23] Petar Kokotović, Hassan K Khalil, and John O'reilly. *Singular perturbation methods in control: analysis and design*. SIAM, 1999.

[24] Karla Kvaternik and Lacra Pavel. An analytic framework for decentralized extremum seeking control. In *2012 American Control Conference (ACC)*, pages 3371–3376. IEEE, 2012.

[25] Tomas Lazna, Petr Gabrlik, Tomas Jilek, and Ludek Zalud. Cooperation between an unmanned aerial vehicle and an unmanned ground vehicle in highly accurate localization of gamma radiation hotspots. *International Journal of Advanced Robotic Systems*, 15(1):1729881417750787, 2018.

[26] Johan Markdahl, Johan Thunberg, and Jorge Goncalves. Almost global consensus on the n-sphere. *IEEE Transactions on Automatic Control*, 63(6):1664–1675, 2017.

[27] Yogeswaran Mohan and SG Ponnambalam. An extensive review of research in swarm robotics. In *2009 World Congress on Nature & Biologically Inspired Computing (NaBIC)*, pages 140–145. IEEE, 2009.

[28] Kwang-Kyo Oh, Myoung-Chul Park, and Hyo-Sung Ahn. A survey of multi-agent formation control. *Automatica*, 53:424–440, 2015.

[29] Erkki Oja. Simplified neuron model as a principal component analyzer. *Journal of mathematical biology*, 15(3):267–273, 1982.

[30] Daniel Pickem, Paul Glotfelter, Li Wang, Mark Mote, Aaron Ames, Eric Feron, and Magnus Egerstedt. The robotarium: A remotely accessible swarm robotics research testbed. In *2017 IEEE International Conference on Robotics and Automation (ICRA)*, pages 1699–1706. IEEE, 2017.

[31] Kazunori Sakurama and Shin-ichiro Nishida. Source seeking by distributed swarm robots with sample variance control. In *2016 American Control Conference (ACC)*, pages 2484–2487. IEEE, 2016.

[32] Avi Turgeman and Herbert Werner. Mission control-combined solutions for source seeking and level curve tracking in a time-varying field. In *2017 American Control Conference (ACC)*, pages 4268–4273. IEEE, 2017.

[33] Jun-Wei Wang, Yi Guo, Muhammad Fahad, and Brian Bingham. Dynamic plume tracking by cooperative robots. *IEEE/ASME Transactions on Mechatronics*, 24(2):609–620, 2019.

[34] Wencen Wu, Dongsik Chang, and Fumin Zhang. A bio-inspired robust 3d plume tracking strategy using mobile sensor networks. In *52nd IEEE Conference on Decision and Control*, pages 4571–4578. IEEE, 2013.

[35] Wencen Wu and Fumin Zhang. A speeding-up and slowing-down strategy for distributed source seeking with robustness analysis. *IEEE Transactions on Control of Network Systems*, 3(3):231–240, 2015.

[36] Shintaro Yoshizawa, Uwe Helmke, and Konstantin Starkov. Convergence analysis for principal component flows. *International Journal of Applied Mathematics and Computer Science*, 11:223–236, 2001.